Climate change-induced greening on the Tibetan Plateau modulated by mountainous characteristics

Hongfen Teng, Zhongkui Luo, Jinfeng Chang, Zhou Shi, Songchao Chen, Yin Zhou, Philippe Ciais, Hanqin Tian

ENVIRONMENTAL RESEARCH
LETTERS

LETTER • OPEN ACCESS

Climate change-induced greening on the Tibetan Plateau modulated by mountainous characteristics

ENVIRONMENTAL RESEARCH
LETTERS

LETTER

Climate change-induced greening on the Tibetan Plateau modulated by mountainous characteristics

Hongfen Teng[1,2], **Zhongkui Luo**[2], **Jinfeng Chang**[2], **Zhou Shi**[2,3,*], **Songchao Chen**[4,5], **Yin Zhou**[2], **Philippe Ciais**[6] and **Hanqin Tian**[7]

[1] School of Environmental Ecology and Biological Engineering, Wuhan Institute of Technology, Wuhan 430205, People's Republic of China
[2] College of Environmental and Resource Sciences, Zhejiang University, Hangzhou 310058, People's Republic of China
[3] State Key Laboratory of Soil and Sustainable Agriculture, Institute of Soil Science, Chinese Academy of Sciences, Nanjing, People's Republic of China
[4] INRA, Unité Infosol, 45075 Orléans, France
[5] UMR SAS, INRA, Agrocampus Ouest, 35042 Rennes, France
[6] Laboratoire des Sciences du Climat et de l'Environnement, CEA-CNRS-UVSQ/IPSL, Université Paris Saclay, 91191 Gif sur Yvette, France
[7] International Center for Climate and Global Change Research, School of Forestry and Wildlife Sciences, Auburn University, Auburn, AL 36849, United States of America
* Author to whom any correspondence should be addressed.

E-mail: shizhou@zju.edu.cn

Keywords: vegetation greenness, spatial variability, climate change, mountainous effects, Tibetan Plateau

Supplementary material for this article is available online

OPEN ACCESS

RECEIVED
15 December 2020

REVISED
11 March 2021

ACCEPTED FOR PUBLICATION
7 May 2021

PUBLISHED
7 June 2021

Abstract

Global terrestrial vegetation is greening, particularly in mountain areas, providing strong feedbacks to a series of ecosystem processes. This greening has been primarily attributed to climate change. However, the spatial variability and magnitude of such greening do not synchronize with those of climate change in mountain areas. By integrating two data sets of satellite-derived normalized difference vegetation index (NDVI) values, which are indicators of vegetation greenness, in the period 1982–2015 across the Tibetan Plateau (TP), we test the hypothesis that climate-change-induced greening is regulated by terrain, baseline climate and soil properties. We find a widespread greening trend over 91% of the TP vegetated areas, with an average greening rate (i.e. increase in NDVI) of 0.011 per decade. The linear mixed-effects model suggests that climate change alone can explain only 26% of the variation in the observed greening. Additionally, 58% of the variability can be explained by the combination of the mountainous characteristics of terrain, baseline climate and soil properties, and 32% of this variability was explained by terrain. Path analysis identified the interconnections of climate change, terrain, baseline climate and soil in determining greening. Our results demonstrate the important role of mountainous effects in greening in response to climate change.

1. Introduction

Understanding changes in vegetation greenness in mountainous areas is of great importance because these changes are associated with a series of ecosystem processes and services, such as carbon and water cycling (Gottfried *et al* 2012, Hagedorn *et al* 2019). Changes in vegetation greenness over time usually consist of an alternating sequence of greening and/or browning, which are defined as statistically significant increases and decreases in vegetation greenness over a period of several years (De Jong *et al* 2012, Chen *et al* 2019a). The effects of climate change, notably global warming or wetting, on vegetation greenness have been widely recognized (Zhu *et al* 2016, Du *et al* 2018, Park *et al* 2020). However, the effects of climate change on greening trends are inconsistent depending on the mountainous characteristics, such as topography, climate and soil properties, which may interact with climate change to regulate vegetation

greenness dynamics (Pugnaire *et al* 2019, Xu *et al* 2020). Identifying the processes underlying the spatial variability of greening under climate change is challenging, particularly in mountainous areas.

The Tibetan Plateau (TP), which is called the 'Third Pole' of the earth with an average elevation of 4000 m (Qiu 2008), has responded more sensitively to climate change than other zones at the same latitude (Duan *et al* 2017, Teng *et al* 2018). Over the past decades, satellite-derived vegetation indices have indicated widespread change on the TP (Shen *et al* 2015a, Zhu *et al* 2016, An *et al* 2018). The long-term changes in vegetation greenness over the TP are recognized to be driven primarily by climate change (Piao *et al* 2014, Zhu *et al* 2016), specifically warming (Qiu 2008) and wetting (Chen *et al* 2013). However, the trend of greening shows great variability on the TP due to the strong vertical zonality of the topography (Anderson *et al* 2020), baseline climate (Shen *et al* 2011), and soil conditions (Kato *et al* 2006). The terrain is a significant regulator of energy and water availability even at fine scales and is very complex on the TP; thus, the terrain may play a vital role in regulating vegetation dynamics (Bolton *et al* 2018, Gao *et al* 2019). The baseline climate plays a key role in the surface energy balance and in modulating the land–climate interactions (Forzieri *et al* 2017), and may therefore impact the widespread greening of the TP. In addition, the heterogeneity of soil nutrient availability and the abiotic soil conditions may lead to profound changes in plant species diversity and community structure (Pugnaire *et al* 2019), ultimately driving diverse greenness dynamics on the TP. The comprehensive impact of climate change, terrain, baseline climate and soil, which influence the permafrost and groundwater, the flow of rainwater into or off the soil, and the heat absorbed by soil, induce extreme local variability of the vegetation composition and structure on the TP (Cheng and Jin 2013, Mu *et al* 2016). Thus, investigating the greening pattern on the TP and the underlying drivers is important for sustainably managing the TP ecosystems and is also important for the land surface energy balance of the region (Zhang *et al* 2013, An *et al* 2018). However, it is still challenging to understand the underlying mechanisms underpinning the spatial variability of greening on the TP.

Long-term remotely sensed measurements of the normalized difference vegetation index (NDVI) have been widely used to indicate changes in large-scale vegetation dynamics and greenness (Huete 2016, Myers-Smith *et al* 2020). Here, we investigate the trend of the growing season NDVI across the TP for the period 1982–2015 using remotely sensed data sets. We present a new method to spatially resample the NDVI record and thus provide a new growing season NDVI data set at a 1 km resolution. Combined with climate records from meteorological stations across the TP, we also disentangle the relative importance of, and interactions among, climate change variables, terrain attributes, baseline climatic characteristics, and soil properties in controlling the spatial variability of the greening trend.

2. Materials and methods

2.1. Satellite-derived NDVI data sets

Two remote sensing data sets, AVHRR GIMMS NDVI3g (hereafter $NDVI_{GIMMS}$) during the period from 1982 to 2015 and SPOT-VGT NDVI (hereafter $NDVI_{SPOT}$) covering the period from 1999 to 2013, were used in this study. $NDVI_{GIMMS}$ is the longest time series NDVI data set and provides information on terrestrial vegetation changes with a spatial resolution of 1/12° (∼8 km) (Tucker *et al* 2005). This data set was compiled by merging segments (data strips) during a half-month period using the maximum value composite (MVC) method. The $NDVI_{SPOT}$ product has been pre-processed by the VEGETATION Processing Centre at the Flemish Institute for Technological Research in Belgium. The spatial resolution of $NDVI_{SPOT}$ is 1 km, and the temporal resolution is 10 days (Maisongrande *et al* 2004). To ensure temporal overlap and equal treatment with $NDVI_{GIMMS}$, the 10 day images were aggregated into monthly MVC.

In this study, we used an empirical orthogonal teleconnections (EOT) model (Appelhans *et al* 2015, Detsch *et al* 2016) to assess the dynamics of the NDVI during 1982–2015 at a 1 km spatial resolution (SI appendix, Processing of NDVI data sets (available online at stacks.iop.org/ERL/16/064064/mmedia)). After that, the new NDVI data set (hereafter $NDVI_{EOT}$) was used in the following analysis. In this study, the EOT analysis was performed using the package *remote* in R 3.6.3 (R Core Team 2020). To minimize the impacts of snow and ice, we considered $NDVI_{EOT}$ within the plant growing season from May to September during 1982–2015 (Shen *et al* 2015b). The mean values of the monthly $NDVI_{EOT}$ (hereafter $NDVI_{mean}$) during the growing season over 1982–2015 were calculated based on the corresponding $NDVI_{EOT}$ values to represent the average of growing season NDVI. To reduce the noise from non-vegetation signals, grid cells with long-term $NDVI_{mean}$ values less than 0.1 over the period 1982–2015 were excluded in this study (Liu *et al* 2016).

2.2. Estimation of long-term NDVI trend

To quantify the long-term trend of growing season vegetation growth, we performed least squares linear regression analysis using the annual growing season $NDVI_{mean}$ as the dependent variable and the year as the independent variable over the period 1982–2015. The slope of the regression (hereafter Tr_{mean}) was then defined as the linear trend of the vegetation

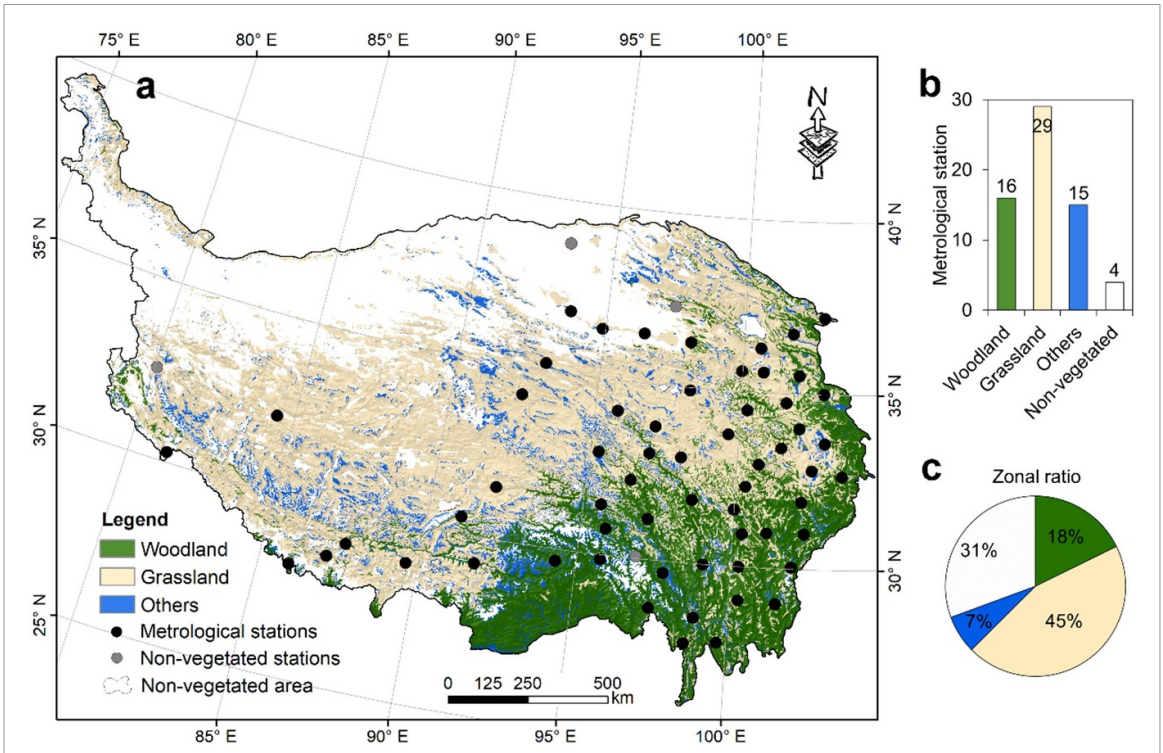

Figure 1. (a) Spatial pattern of meteorological stations based on an ecosystem map of the Tibetan Plateau (TP) from the 1:1000 000 Vegetation Atlas of China (Editorial Board of Vegetation Map of China) provided by the Data Center for Resources and Environmental Sciences, Chinese Academy of Sciences (RESDC) (www.resdc.cn). (b) Number of meteorological stations in each of the ecosystem types analyzed in this study. (c) Zonal statistics of each ecosystem based on the ecosystem map. The non-vegetated areas with growing season NDVI lower than 0.10 are not considered in this study.

growth over the growing season. Positive and negative values of Tr_{mean} over time can be referred to as *greening* and *browning*, respectively. The spatial patterns of the temporal trends in each data set were calculated using least squares linear regression for each grid. All the data calculations were accomplished using the function *lm()* in R 3.6.3 (R Core Team 2020).

2.3. Identifying possible driving factors

2.3.1. Climate variables

There were 64 meteorological stations, which contained daily climate variables of precipitation, temperature and evaporation, provided by the China Meteorological Administration over the TP during the study period 1982–2015. Among these meteorological stations, four had a corresponding $NDVI_{mean}$ less than 0.1 during the study period, and were excluded from this study. Thus, 60 meteorological stations were used in the following analysis (figure 1).

In this study, ten baseline climate variables, which determined a reference point for climate change based on the average climate over a 33 year period (1982–2015) based on monthly precipitation, temperature and evaporation data sets, were calculated from daily records from 60 meteorological stations over the TP. They included the average annual total precipitation (P_{re}), average total precipitation in the growing season (P_{re_gs}), average annual mean temperature (T_{mp}), average mean temperature in the growing season (T_{mp_gs}), average annual minimum temperature (T_{mn}), average minimum temperature in the growing season (T_{mn_gs}), average annual maximum temperature (T_{mx}), average maximum temperature in the growing season (T_{mx_gs}), average annual total evaporation (E_{vp}), and average total evaporation in the growing season (E_{vp_gs}). The corresponding ten climate change variables, which represented the long-term trend of climate dynamics (Tr_{Pre}, Tr_{Pre_gs}, Tr_{Tmp}, Tr_{Tmp_gs}, Tr_{Tmn}, Tr_{Tmn_gs}, Tr_{Tmx}, Tr_{Tmx_gs}, Tr_{Evp}, Tr_{Evp_gs}), were also calculated (table S1). All ten climate change variables were quantified by performing least squares linear regression analysis using climate data sets as the dependent variable and year as the independent variable over the period 1982–2015. The regression slopes of the linear regression models were identified as the trends of the corresponding climate change variables (table S1).

Since the ten baseline climate variables and ten climate change variables were highly correlative (figures S2(a) and (d)), we used principal component analysis (PCA) to summarize/reduce the informative features and control for autocorrelations between these variables. We performed PCA on all variables reflecting the baseline climate variables ($n = 10$) and climate change ($n = 10$) to analyze the variation in baseline climate (PCb) and climate change (PCc). Based on the PCA results, three PCbs (PCb1 to PCb3)

that explained 97.25% of the baseline climate variance and six PCcs (PCc1 to PCc6) that explained 96.08% of the variance in the assessed climate change factors were used in the following analysis (figure S2).

2.3.2. Terrain

At each of the 60 meteorological stations, seven terrain attributes, including the digital elevation model (DEM), slope, aspect, curvature (Curv), topographic wetness index (TWI), multiresolution index of valley bottom flatness (MrVBF), and terrain ruggedness index (TRI), were extracted from the 3 arcsecond (approximately 90 m) grid Shuttle Radar Topography Mission DEM (SI appendix, Explanation of terrain attributes).

2.3.3. Soil attributes

Maps of bulk density (BD), total nitrogen (TOTN), soil content (sand, silt and clay), effective cation exchange capacity (ECEC), total exchangeable bases (TEB), and available water capacity (TAWC) were obtained from a 30 arcsecond raster database of the harmonized soil property values for the world (WISE30sec) (Batjes 2016). Soil maps of pH (Chen *et al* 2019b) and soil organic matter (SOM) (Liang *et al* 2019) were produced using soil samples, environmental variables, and digital soil mapping techniques. In this study, the ten soil attributes mentioned above were extracted at the 60 meteorological station locations for the following analysis.

2.3.4. Ecosystem types

The ecosystem types were identified according to the vegetation map of the TP that was obtained from the Data Center for Resources and Environmental Sciences, Chinese Academy of Sciences (RESDC) (www.resdc.cn). The vegetation map was produced from a digitized 1:1000 000 Vegetation Atlas of China (Chinese Academy of Sciences 2001). In the vegetation map, four vegetation types related to forest (coniferous forest, coniferous and broad-leaved mixed forest, broad-leaved forest, and shrub) were classified as woodland ecosystems; three vegetation types belonging to grassland (steppe, herbs and meadow) were classified as woodland ecosystems. Other vegetation types, including alpine vegetation, cultivated vegetation desert and others, were classified as other ecosystems (figure 1).

2.4. Disentangling the contributions of driving factors on the spatial variability of the greening trends

We explored the variability of the relationships between indicators (i.e. climate change, terrain, baseline climate and soil) and the response variable (Tr_{mean}) by using a linear mixed-effects model (LMM) (Qie *et al* 2017) at the 60 meteorological stations. The LMM contains two components: a fixed effect (the explanatory variables) and random effects. Hypotheses were made prior to assessing the contributions of climate change, terrain, baseline climate and soil to the greening variation. First, we assumed that climate change impacted greening. Second, we assumed that the impact of climate change on the spatial variability of the greening trend was modulated by terrain, baseline climate and soil attributes. Third, we assumed that terrain characteristics amplified the spatial variability of the greening.

We built three sets of LMMs to examine these hypotheses. The first set of LMMs used the six climate change variables (PCc1 to PCc6, figure S2) as explanatory variables and Tr_{mean} as the response variable to describe the response variable of the greening trend. The second set of LMMs used the variables of climate change (PCc1 to PCc6), terrain, baseline climate (PCb1 to PCb3) and soil as explanatory variables. The third set of LMMs was used similarly to the second set of LMMs, but without the terrain attribute.

Ecosystem types were treated as a random effect, allowing each ecosystem type to have a separate intercept in all sets of LMMs. The predicted greening rates by the three sets of LMMs driven by the identified variables mentioned above were compared with the corresponding modeled greening rates. The LMM enabled the estimation of the assessed RMSE of an explanatory variable (i.e. climate change, terrain, baseline climate and soil in this study) compared with other variables that were considered. In this study, we used the RMSE value to evaluate the relative importance of a given variable in the LMM (SI appendix, Relative importance of variables), and also used the resulting coefficient of determination (R^2) to present the explanation rate of the model. The LMMs were used at the locations of the 60 meteorological stations using the package *nlme* in R 3.6.3 (R Core Team 2020).

2.5. Partial least squares—path modeling (PLS-PM)

We applied PLS-PM with four latent variables, namely, climate change, terrain, baseline climate and soil, to assess their direct/indirect effects on the variability of Tr_{mean}. The latent variables were reflected by indicators. For example, for the latent variable 'climate change,' we considered six indicators: PCc1 to PCc6. In the PLS-PM, the loading of each latent variable was the key to estimating the variable scores and was calculated as the correlation between a latent variable and its indicators. An iterative algorithm was used to estimate the loadings until the convergence of the loadings was reached to maximize the explained variance of the dependent variables (both latent and indicator variables) (Luo *et al* 2019). The R^2 values of the endogenous latent variables indicated the amount of variance in the endogenous latent variable explained by its independent latent variables. The

result of the path coefficient can be positive or negative. A negative path coefficient means that increasing the causal variable causes a decrease in the dependent variable if all other causal variables are held constant.

Using PLS-PM, we explored how the greening trend responded to climate change, terrain, baseline climate and soil, and we also investigated the interactions among these variables. We first assumed that climate change, terrain, baseline climate and soil directly impact the spatial variability of the greening trend. Second, we assumed that these variables have indirect impacts on the spatial variability of the greening trend through their interactions with each other. We also tested the assumptions based on the variables without terrain (climate change, baseline climate and soil). The PLS-PM was performed using the package *plspm* in R 3.6.3 (R Core Team 2020).

3. Results

3.1. Climate change over the past decades on the TP

Figure 2 shows the long-term annual total precipitation, average mean temperature and annual total evaporation as well as their corresponding trends during 1982–2015. During the past three decades, the TP has experienced a warming trend based on the comparison of time series annual average temperature on the whole TP (0.05 °C yr^{-1}, $p < 0.0001$), woodland ecosystem (0.04 °C yr^{-1}, $p < 0.0001$) and grassland ecosystem (0.07 °C yr^{-1}, $p < 0.0001$) (figure 2). Based on the records of the 60 meteorological stations, the total annual precipitation showed interannual variation with an insignificant trend during 1982–2015 (0.13 mm yr^{-1}, $p = 0.8206$). Woodland ecosystem, however, showed a significant decreasing trend of annual total precipitation over the study period (−1.67 mm yr^{-1}, $p = 0.0415$). The annual total evaporation showed a universal decreasing trend over the whole TP, woodland ecosystem, and grassland ecosystem (figure 2).

3.2. Greening on the TP

The growing season $NDVI_{EOT}$ of the time series grid cells at a 1 km resolution shows a mean value of $NDVI_{mean}$ of 0.343, with an increasing trend of 0.011 per decade (i.e. greening, $p < 0.0001$) across the whole TP during the period 1982–2015 (figure 3(c)). In general, the NDVI increases from the very dry western TP to the wetter eastern TP. At the pixel level, $NDVI_{mean}$ shows great spatial variability, ranging from 0.10 to 0.83 (figure 3(a)). A 91% proportion of the vegetated land over the TP exhibits greening (i.e. $Tr_{mean} > 0$, $p < 0.0001$), and only 9% experiences browning ($p < 0.0001$), that is, a decrease in $NDVI_{mean}$ (figure 3(b)). Woodland ecosystems, which grow at lower altitudes (1706 ∼ 4440 m), have a higher $NDVI_{mean}$ value (0.514) (figure 3(d)) and show more rapid and significant greening rates (0.013 per decade, $p = 0.0003$) than the average value for the whole TP. Grassland ecosystems, which account for 45% of the total TP (figure 1(c)), show a lower greening rate than the whole TP (0.010 per decade, $p < 0.0001$), with an $NDVI_{mean}$ value of 0.286 (figure 3(e)).

3.3. Association of greening with climate change only

The LMM results suggested that climate change explains only 26% of the spatial variability of greening trends ($R^2 = 0.26$) (figure 4(a)). The random intercepts for woodland and grassland ecosystems were 0.08 ($\times 10^{-10}$) and 0.04 ($\times 10^{-10}$), respectively (table S2). Among the indicators of climate change, PCc4, which had a high correlation with Tr_{Tmx_gs} over 1982–2015 based on the PCA results (correlation = 0.55, figure S2(f)), showed significant correlation with the greening trend (coefficient = −3.23, table S2).

3.4. Greening modulated by terrain, baseline climate and soil properties

In addition to climate change, we introduce terrain, baseline climate and soil variables (table S1) into the LMM to test the hypothesis that these factors modulate the impact of climate change on the spatial variability of greening rates. We find that variables of terrain, baseline climate and soil can explain another 58% of the greening trend variability ($R^2 = 0.26$ for climate change alone versus $R^2 = 0.84$ for all variables together). Among these variables, terrain can help explain more than 32% of the variability ($R^2 = 0.52$ with all variables except terrain) (figure 4(a)).

The results regarding the relative influence of the LMM, which includes all environmental variables, suggest that terrain is the most important variable in terms of explaining the spatial variation in greening trends (relative importance = 42%). Altitude has been found to be the most important indicator within terrain variables in driving the spatial variation in greening trends (relative importance = 14%) (figure 4(b)). PCb1, which was mainly correlated with temperature (figure S2(c)), showed the highest contribution in the baseline climate to explaining the spatial variance of greening trends (relative importance = 13%). Overall, the contribution of soil to explaining the variance of greening was comparable to that of other variables (relative importance = 28%). According to our results, the ECEC showed the highest relative importance value (8%) for the greening trend among the soil attributes (figure 4(b)).

3.5. Interconnections between greening trend and its drivers

PLS-PM suggests that climate change is directly and negatively correlated with the spatial variability of greening trends over the whole TP (correlation coefficients = −0.40) (figure 5(a)). However, the correlation between climate change and greening could

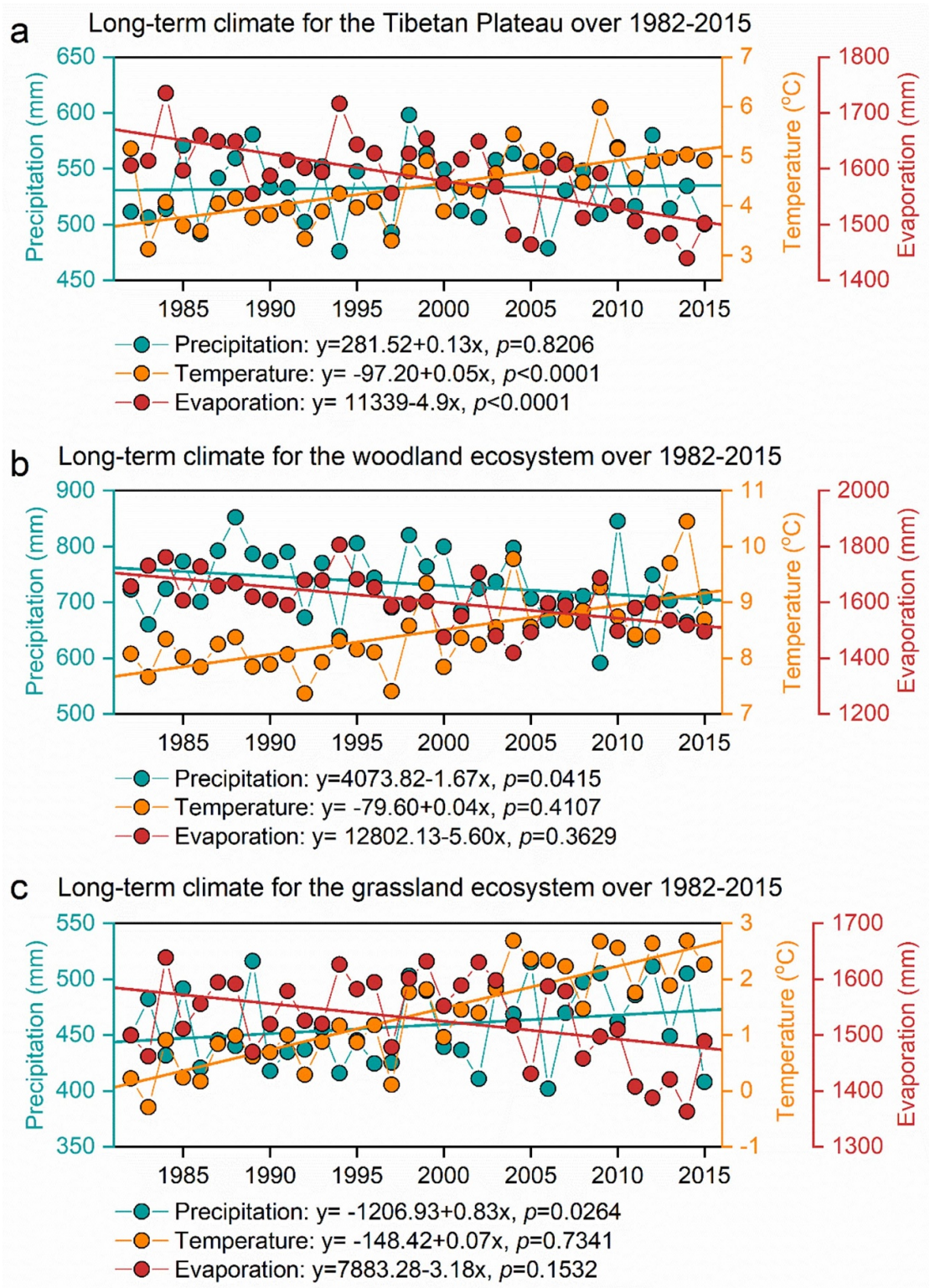

Figure 2. Comparisons of long-term annual total precipitation, average mean temperature, and total evaporation over (a) the TP, (b) woodland ecosystem, and (c) grassland ecosystem based on average values at the 60 meteorological stations over 1982–2015. Regression lines are overlaid for each climate variable and corresponding regression equations are reported in the label.

be different among ecosystems, which is 0.57 in the woodland and −0.11 in the grassland (figures 5(b) and (c)). According to the loading score of each indicator to the corresponding variable, PCc1, which was mainly correlated with temperature (figure S2(c)), was a more powerful indicator of climate change for the model over the whole TP and woodland (loading score = 0.76 and 0.89, respectively). However, PCc2, which was mainly correlated with evaporation (figure S2(c)), was a more powerful indicator of climate change for the grassland (loading score = −0.96) (table S3). Climate change also indirectly affects the

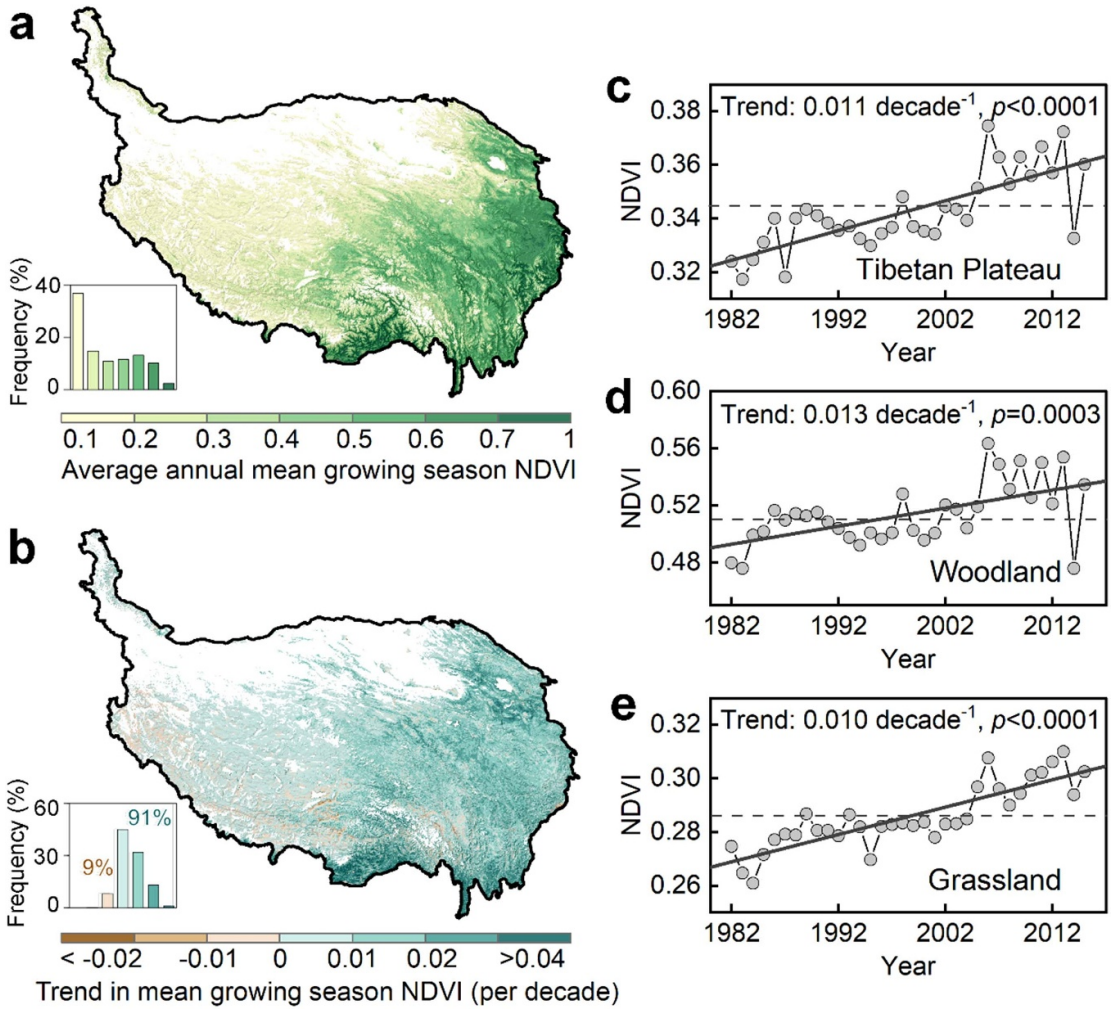

Figure 3. Spatial pattern of (a) average annual mean growing season NDVI ($NDVI_{mean}$) and (b) the trend in $NDVI_{mean}$ (Tr_{mean}) for 1982–2015. White pattern indicates areas with a multiyear average growing season NDVI less than 0.1. Comparisons of long-term trends in annual mean growing season NDVI over the different ecosystem types across the TP based on the zonal statistics for (c) the whole TP, (d) woodland ecosystem, and (e) grassland ecosystem over the growing season (May to September) during 1982–2015. The statistically insignificant regions ($p > 0.05$) are masked out from the statistics. The black and solid regression lines are overlaid and corresponding regression equations are reported in the labels. The average values of mean growing season NDVI for each ecosystem are shown by gray and dashed lines.

greening trend through its impact on soils (correlation coefficients = 0.19) (figure 5(a)). Baseline climate, which was mainly derived by temperature on PCb2 (loading scores = −0.77, figure S2(f), table S3), was shown to have a higher direct contribution than climate change in terms of explaining the variance of greening (correlation coefficient = −0.72) (figure 5(a)).

Terrain, which is mainly reflected by the TRI and TWI (loading scores in the path analysis are −0.90 and 0.90, respectively; table S4), had direct and negative control on the variability of greenness (correlation coefficient = −0.24) (figure 5(d)). This finding could be amplified over woodland ecosystems, with a direct correlation coefficient of −0.65 between terrain and greening (figure 5(e)). The terrain also had an indirect relationship with the greening rate via all hypothesized pathways, including those involving climate change, baseline climate and soil (figure 5). The direct impact of climate change on greening could be strengthened over woodland and grassland when the terrain attributes were included in the path analysis (figures 5(e) and (f)).

4. Discussion

As expected, climate change has a significant direct effect on the spatial variability of greening trends. The finding of a high correlation between temperature and vegetation dynamics (table S2 and figure S2(f)) was in line with previous research showing that the vegetation phenology at high latitudes is primarily determined by temperature (Shen *et al* 2016). However, the temperature increase may have variable effects on greening among ecosystems. In this study, woodland ecosystem experienced a relatively rapid greening trend during the warming period over 1982–2015. The increasing temperature, which

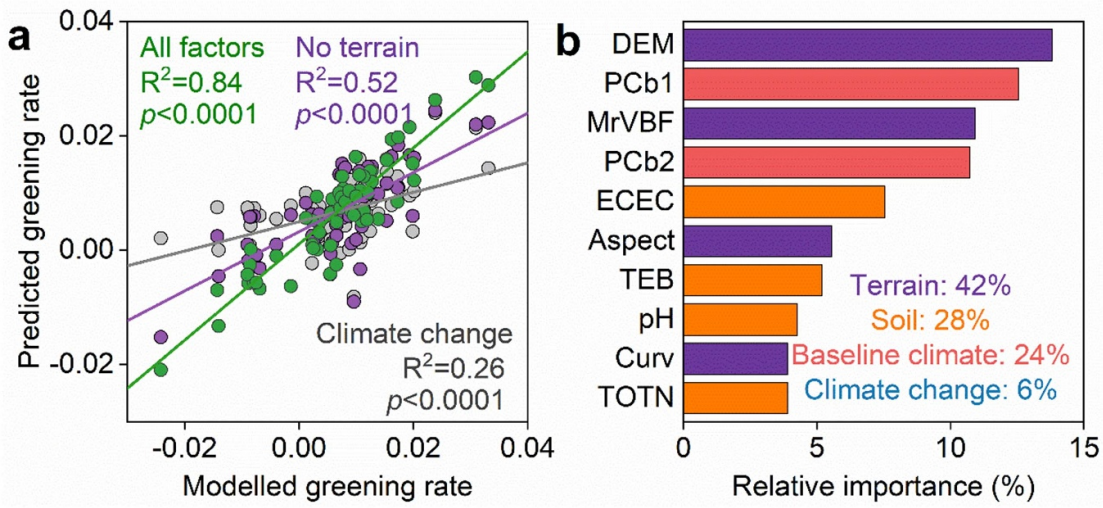

Figure 4. (a) Performance of the linear mixed-effects models (LMMs) in predicting greening rates during 1982–2015 using three sets of predictors. The first set of LMMs used climate change variables (PCc1 to PCc6) as predictors, the second set of LMMs selected climate change (PCc1 to PCc6), baseline climate (PCb1 to PCb3), terrain, and soil variables as predictors, and the third set of LMMs used similar predictors to the second set but without terrain. (b) First ten important variables of predictors in the second set of LMMs. The blue bars show indicators in climate change, the purple bars show indicators in terrain, the pink bars show indicators in baseline climate, and the orange bars show indicators in soil. All sets of LMMs were employed based on the values at 60 meteorological stations.

primarily contributed to the indicator of PCc1 in the climate change variable, promoted the greening over the woodland ecosystem (figure 5(b), table S3, figure S2(f)), indicating that warmer temperature may lead to an extended growing season for temperate forests due to earlier greenup and delayed senescence (Hwang *et al* 2014). However, increasing temperature will have a negative impact on the greening over the grassland ecosystem. Warming over the TP induced an increased preseason precipitation and corresponding reduced precipitation during the growing season. The deficient sunshine intensity and duration of preseason, and the drought stress induced by dramatic increases in temperature and inadequate precipitation during the growing season, could counteract early spring carbon assimilation (Angert *et al* 2005) and increase vegetation mortality (Adams *et al* 2009). Accelerated leaf senescence associated with drought stress along with warming has been studied specifically in grasslands (Rivero *et al* 2007), for which chemical mechanisms are largely known.

Moreover, climate change not only favors the rapid growth of plants and controls the structure and function of ecosystems but also accelerates permafrost thawing throughout the TP (Chen *et al* 2013). In past decades, the mean annual permafrost temperatures at a depth of 6.0 m increased by 0.12 °C–0.67 °C (Wu and Zhang 2008). Such permafrost degradation caused rapid soil carbon loss through the efflux of CH_4 and CO_2. In turn, the decomposition of soil organic carbon over these areas has accelerated with climate warming (Chen *et al* 2013). On the other hand, a changing climate has the potential to alter the composition of plant and soil communities and the interactions between them. The interactions among plants and their associated abiotic soils, which are termed plant–soil feedbacks, can lead to complex feedbacks that regulate plant community dynamics and ecosystem processes (Pugnaire *et al* 2019).

There is growing evidence that the impact of climate change on the trend of vegetation greenness can be amplified by terrain attributes (Liu *et al* 2013, An *et al* 2018, Radula *et al* 2018). The influence of elevation-dependent warming on the vegetation dynamics in mountainous environments has also been documented, revealing that warming is more rapid at higher elevations (Mountain Research Initiative EDW Working Group 2015, Xu *et al* 2020). For instance, warming promotes seedling establishment and vegetation infilling (Du *et al* 2018) and induces the upward migration of the treeline on the TP. The terrain also causes localized changes in soil moisture and soil temperature. The steepness, shape and slope of an area affect the flow of rainwater into or off the soil as well as the amount of heat absorbed by the soil. Moreover, the structure and function of ecosystems vary significantly with climate driven by fine-scale variations in topography. It is usually assumed that the spatial variability of the greening trend over the mid- and high-latitude forest phenology is primarily determined by temperature, while seasonal rainfall is a more important factor for the interannual vegetation greenness dynamics in arid and semiarid grassland regions (figure 2) (Hwang *et al* 2014).

Baseline climate also has an impact on the greenness trend through its relationship with climate change, soil, and vegetation type (figure 5). At higher latitudes, plants slow or postpone developmental

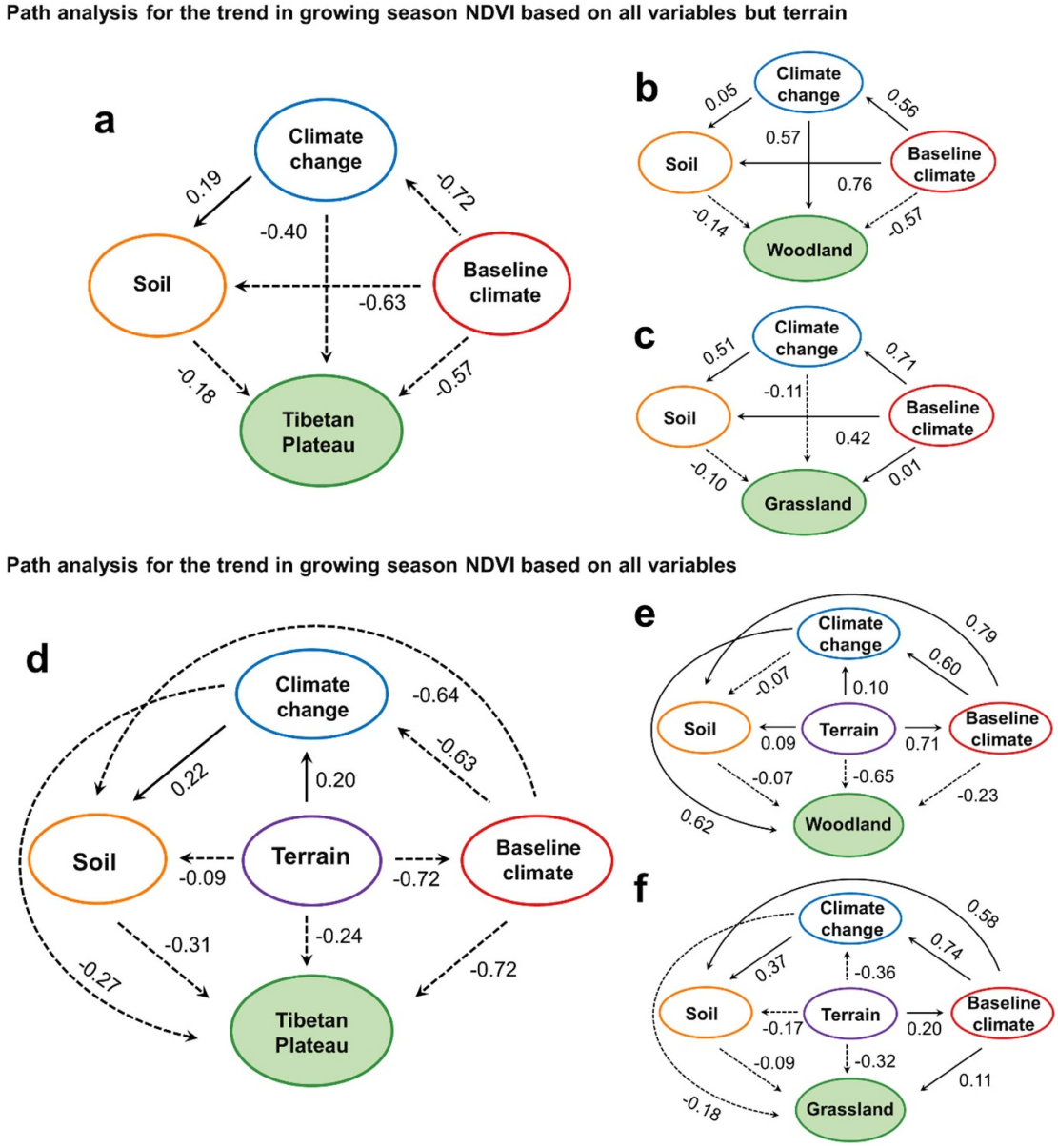

Figure 5. Results of path analysis on the direction and magnitude of the effects of latent variable climate change and climate, and soil for Tr_{mean} during 1982–2015 for (a) the whole TP, (b) woodland ecosystem, and (c) grassland ecosystem. Path analysis on the direction and magnitude of the effects of latent variable climate change, climate, terrain and soil for Tr_{mean} during 1982–2015 for (d) the whole TP, (e) woodland ecosystem, and (f) grassland ecosystem. Continuous arrows indicate positive relationships. Dashed arrows indicate negative relationships. Numbers in parentheses show the direct correlation coefficients between the latent variables. Path analysis was performed based on the values at 60 meteorological stations.

processes to mitigate the high risk of freezing injury at very low temperatures (Shen *et al* 2016). Frozen soil water under low temperatures could limit water absorption by alpine vegetation roots. The dominant enhancing effect of the increasing minimum temperature was likely caused by the reduction in low-temperature constraints on alpine plants, which promoted vegetation growth. In this study, the grassland with a higher average temperature (i.e. meadow) showed a higher greening rate than that in a colder environment (i.e. steppe) (figures 2 and 4). Moreover, the combined effects of changes in snow depth and cloud cover in response to the increase in CO_2 concentrations result in greater surface heat storage in high-mountain regions and therefore amplify the warming rate with elevation on the TP (Palazzi *et al* 2017). The implications for the combination of cloud radiation and snow albedo feedbacks and the increases in water vapor content in the atmosphere can thus affect the greening trend (Mountain Research Initiative EDW Working Group 2015, Yan *et al* 2016).

5. Conclusion

This study used multiple data sources and approaches to evaluate the greening trend of the TP vegetation and revealed the drivers of the variation in this

greening. The findings of this study have several important implications. First, our results suggest an overall greening trend over the TP in recent decades. Second, the variability of greening in recent decades has been driven not only by climate change but also by terrain, baseline climate and soil. Finally, the interconnections of climate change, terrain, baseline climate and soil need to be considered in understanding and predicting the vegetation dynamics over the TP. The methods and logic developed here could aid understanding of the influence of climate change on terrestrial vegetation and toward improving the simulation of future vegetation dynamics.

Data availability statement

All data that support the findings of this study are included within the article (and any supplementary files).

Acknowledgments

This research was supported by the National Natural Science Foundation of China (No. 41901055, 41930754). We thank all the people involved in climate analysis and vegetation modeling related to this study.

ORCID iDs

Hongfen Teng https://orcid.org/0000-0003-4384-9402
Zhongkui Luo https://orcid.org/0000-0002-6744-6491
Jinfeng Chang https://orcid.org/0000-0003-4463-7778
Zhou Shi https://orcid.org/0000-0003-3914-5402
Songchao Chen https://orcid.org/0000-0003-1245-0482
Philippe Ciais https://orcid.org/0000-0001-8560-4943
Hanqin Tian https://orcid.org/0000-0002-1806-4091

References

Adams H D, Guardiola-Claramonte M, Barron-Gafford G A, Villegas J C, Breshears D D, Zou C B, Troch P A and Huxman T E 2009 Temperature sensitivity of drought-induced tree mortality portends increased regional die-off under global-change-type drought *Proc. Natl Acad. Sci. USA* **106** 7063–6

An S, Zhu X, Shen M, Wang Y, Cao R, Chen X, Yang W, Chen J and Tang Y 2018 Mismatch in elevational shifts between satellite observed vegetation greenness and temperature isolines during 2000–2016 on the Tibetan Plateau *Glob. Change Biol.* **24** 5411–25

Anderson K, Fawcett D, Cugulliere A, Benford S, Jones D and Leng R 2020 Vegetation expansion in the subnival Hindu Kush Himalaya *Glob. Change Biol.* **26** 1608–25

Angert A, Biraud S, Bonfils C, Henning C C, Buermann W, Pinzon J, Tucker C J and Fung I 2005 Drier summers cancel out the CO_2 uptake enhancement induced by warmer springs *Proc. Natl Acad. Sci. USA* **102** 10823–7

Appelhans T, Detsch F and Nauss T 2015 Remote: empirical orthogonal teleconnections in R *J. Stat. Softw.* **65** 1–19

Batjes N H 2016 Harmonized soil property values for broad-scale modelling (WISE30sec) with estimates of global soil carbon stocks *Geoderma* **269** 61–8

Bolton D K, Coops N C, Hermosilla T, Wulder M A and White J C 2018 Evidence of vegetation greening at alpine treeline ecotones: three decades of Landsat spectral trends informed by lidar-derived vertical structure *Environ. Res. Lett.* **13** 084022

Chen C *et al* 2019a China and India lead in greening of the world through land-use management *Nat. Sustain.* **2** 122–9

Chen H *et al* 2013 The impacts of climate change and human activities on biogeochemical cycles on the Qinghai-Tibetan Plateau *Glob. Change Biol.* **19** 2940–55

Chen S C, Liang Z, Webster R, Zhang G, Zhou Y, Teng H, Hu B, Arrouays D and Shi Z 2019b A high-resolution map of soil pH in China made by hybrid modelling of sparse soil data and environmental covariates and its implications for pollution *Sci. Total Environ.* **655** 273–83

Cheng G D and Jin H J 2013 Permafrost e águas subterrâneas no planalto de Qinghai-Tibete e no nordeste da China *Hydrogeol. J.* **21** 5–23

Chinese Academy of Sciences 2001 1:1 000 000 Vegetation Atlas of China. (Beijing: Science Press)

De Jong R, Verbesselt J, Schaepman M E and De Bruin S 2012 Trend changes in global greening and browning: contribution of short-term trends to longer-term change *Glob. Change Biol.* **18** 642–55

Detsch F, Otte I, Appelhans T, Hemp A and Nauss T 2016 Seasonal and long-term vegetation dynamics from 1-km GIMMS-based NDVI time series at Mt. Kilimanjaro, Tanzania *Remote Sens. Environ.* **178** 70–83

Du H B, Liu J, Li M-H, Büntgen U, Yang Y, Wang L, Wu Z and He H S 2018 Warming-induced upward migration of the alpine treeline in the Changbai Mountains, northeast China *Glob. Change Biol.* **24** 1256–66

Duan J P, Esper J, Büntgen U, Li L, Xoplaki E, Zhang H, Wang L, Fang Y and Luterbacher J 2017 Weakening of annual temperature cycle over the Tibetan Plateau since the 1870s *Nat. Commun.* **8** 14008

Forzieri G, Alkama R, Miralles D G and Cescatti A 2017 Satellites reveal contrasting responses of regional climate to the widespread greening of Earth *Science* **356** 1140–4

Gao M D, Piao S, Chen A, Yang H, Liu Q, Fu Y H and Janssens I A 2019 Divergent changes in the elevational gradient of vegetation activities over the last 30 years *Nat. Commun.* **10** 10

Gottfried M *et al* 2012 Continent-wide response of mountain vegetation to climate change *Nat. Clim. Change* **2** 111–5

Hagedorn F, Gavazov K and Alexander J M 2019 Above- and belowground linkages shape responses of mountain vegetation to climate change *Science* **365** 1119–23

Huete A 2016 Vegetation's responses to climate variability *Nature* **531** 181–2

Hwang T, Band L E, Miniat C F, Song C, Bolstad P V, Vose J M and Love J P 2014 Divergent phenological response to hydroclimate variability in forested mountain watersheds *Glob. Change Biol.* **20** 2580–95

Kato T, Tang Y, Gu S, Hirota M, Du M, Li Y and Zhao X 2006 Temperature and biomass influences on interannual changes in CO_2 exchange in an alpine meadow on the Qinghai-Tibetan Plateau *Glob. Change Biol.* **12** 1285–98

Liang Z Z, Chen S, Yang Y, Zhao R, Shi Z and Viscarra Rossel R A 2019 National digital soil map of organic matter in topsoil and its associated uncertainty in 1980's China *Geoderma* **335** 47–56

Liu H, Tian F, Hu H C, Hu H P and Sivapalan M 2013 Soil moisture controls on patterns of grass green-up in Inner

Mongolia: an index based approach *Hydrol. Earth Syst. Sci.* **17** 805–15
Liu Q, Fu Y H, Zeng Z, Huang M, Li X and Piao S 2016 Temperature, precipitation, and insolation effects on autumn vegetation phenology in temperate China *Glob. Change Biol.* **22** 644–55
Luo Z K, Wang G C and Wang E L 2019 Global subsoil organic carbon turnover times dominantly controlled by soil properties rather than climate *Nat. Commun.* **10** 3688
Maisongrande P, Duchemin B and Dedieu G 2004 VEGETATION/SPOT: an operational mission for the Earth monitoring; presentation of new standard products *Int. J. Remote Sens.* **25** 9–14
Mountain Research Initiative EDW Working Group 2015 Elevation-dependent warming in mountain regions of the world *Nat. Clim. Change* **5** 424–30
Mu C C, Zhang T, Zhang X, Li L, Guo H, Zhao Q, Cao L, Wu Q and Cheng G 2016 Carbon loss and chemical changes from permafrost collapse in the northern Tibetan Plateau *J. Geophys. Res. Biogeosci.* **121** 1781–91
Myers-Smith I H *et al* 2020 Complexity revealed in the greening of the Arctic *Nat. Clim. Change* **10** 106–17
Palazzi E, Filippi L and Von Hardenberg J 2017 Insights into elevation-dependent warming in the Tibetan Plateau-Himalayas from CMIP5 model simulations *Clim. Dyn.* **48** 3991–4008
Park H, Jeong S and Penuelas J 2020 Accelerated rate of vegetation green-up related to warming at northern high latitudes *Glob. Change Biol.* **26** 6190–202
Piao S L *et al* 2014 Evidence for a weakening relationship between interannual temperature variability and northern vegetation activity *Nat. Commun.* **5** 5018
Pugnaire F I, Morillo J A, Peñuelas J, Reich P B, Bardgett R D, Gaxiola A, Wardle D A and Van Der Putten W H 2019 Climate change effects on plant–soil feedbacks and consequences for biodiversity and functioning of terrestrial ecosystems *Sci. Adv.* **5** eaaz1834
Qie L *et al* 2017 Long-term carbon sink in Borneo's forests halted by drought and vulnerable to edge effects *Nat. Commun.* **8** 1966
Qiu J 2008 China: the third pole *Nature* **454** 393–6
R Core Team 2020 R: a language and environment for statistical computing *R Foundation for Statistical Computing* (Vienna)
Radula M W, Szymura T H and Szymura M 2018 Topographic wetness index explains soil moisture better than bioindication with Ellenberg's indicator values *Ecol. Indic.* **85** 172–9
Rivero R M, Kojima M, Gepstein A, Sakakibara H, Mittler R, Gepstein S and Blumwald E 2007 Delayed leaf senescence induces extreme drought tolerance in a flowering plant *Proc. Natl Acad. Sci. USA* **104** 19631–6
Shen M G *et al* 2015b Evaporative cooling over the Tibetan Plateau induced by vegetation growth *Proc. Natl Acad. Sci. USA* **112** 9299–304
Shen M G, Piao S, Chen X, An S, Fu Y H, Wang S, Cong N and Janssens I A 2016 Strong impacts of daily minimum temperature on the green-up date and summer greenness of the Tibetan Plateau *Glob. Change Biol.* **22** 3057–66
Shen M G, Piao S, Dorji T, Liu Q, Cong N, Chen X, An S, Wang S, Wang T and Zhang G 2015a Plant phenological responses to climate change on the Tibetan Plateau: research status and challenges *Natl Sci. Rev.* **2** 454–67
Shen M G, Tang Y H, Chen J, Zhu X L and Zheng Y H 2011 Influences of temperature and precipitation before the growing season on spring phenology in grasslands of the central and eastern Qinghai-Tibetan Plateau *Agric. Forest Meteorol.* **151** 1711–22
Teng H F, Liang Z, Chen S, Liu Y, Viscarra Rossel R A, Chappell A, Yu W and Shi Z 2018 Current and future assessments of soil erosion by water on the Tibetan Plateau based on RUSLE and CMIP5 climate models *Sci. Total Environ.* **635** 673–86
Tucker C J, Pinzon J E, Brown M E, Slayback D A, Pak E W, Mahoney R, Vermote E F and El Saleous N 2005 An extended AVHRR 8-km NDVI dataset compatible with MODIS and SPOT vegetation NDVI data *Int. J. Remote Sens.* **26** 4485–98
Wu Q B and Zhang T J 2008 Recent permafrost warming on the Qinghai-Tibetan plateau *J. Geophys. Res. Atmos.* **113** D13108
Xu S, Yu Z, Lettenmaier D P, McVicar T R and Ji X 2020 Elevation-dependent response of vegetation dynamics to climate change in a cold mountainous region *Environ. Res. Lett.* **15** 094005
Yan L, Liu Z, Chen G, Kutzbach J E and Liu X 2016 Mechanisms of elevation-dependent warming over the Tibetan plateau in quadrupled CO_2 experiments *Clim. Change* **135** 509–19
Zhang G L, Zhang Y J, Dong J W and Xiao X M 2013 Green-up dates in the Tibetan Plateau have continuously advanced from 1982 to 2011 *Proc. Natl Acad. Sci. USA* **110** 4309–14
Zhu Z C *et al* 2016 Greening of the Earth and its drivers *Nat. Clim. Change* **6** 791–6